PAPER

Check for updates

Prospects of surfactant assisted dispersive liquid–liquid microextraction for the selective extraction of silver and titanium dioxide nanoparticles from tap water and determination by spICP-MS

Ana Justo-Vega, Raquel Domínguez-González, Pilar Bermejo-Barrera [ID] *
and Antonio Moreda-Piñeiro [ID]

The widespread use of inorganic nanoparticles (NPs), especially silver (Ag) and titanium dioxide (TiO$_2$) NPs, has led to growing concern about their impact on human health and the environment. Inorganic nanoparticles are present in a large variety of products including cosmetics, foodstuffs, and medical goods, and NPs releasing from consumers' products into the environment can be therefore expected. Because of the low concentration levels of NPs in water, special care must be taken when developing new reliable analytical methods. In the current research, the possibilities of surfactant-assisted dispersive liquid–liquid microextraction (SADLLME) in combination with single-particle inductively coupled plasma mass spectrometry (spICP-MS) have been explored/discussed. Optimum conditions for the pre-concentration of TiO$_2$ NPs and Ag NPs were 10 mL of water sample, 1.0 mL of the Triton X114/1,2-dichloroethane (49 : 1) mixture, vortexing at 1500 rpm for 30 s, and centrifugation at 3500 rpm for 5 min. The collected organic phase was finally diluted to 1–2 mL with 1% (w/v) glycerol, leading to an enrichment factor within the 5–10 range. The developed procedure (sample pre-treatment and spICP-MS) led to a size detection limit (5σ criteria) of 65.8 and 16.7 nm for TiO$_2$ NPs and Ag NPs, respectively. The limit of detection in number concentration was 6.06×10^6 L^{-1} for Ag NPs and 2.85×10^6 L^{-1} for TiO$_2$ NPs, whereas the limit of detection for dissolved Ag and Ti mass concentrations was found to be 0.435 and 9.82 ng L^{-1}, respectively. The operational simplicity, low cost and less consumption of organic solvents make SADLLME a greener and faster choice compared to classical liquid–liquid extraction techniques.

1. Introduction

The scientific interest in nanomaterials (NMs), mainly in inorganic nanoparticles (NPs), has exponentially increased since the early 2000s. Due to the unique and outstanding properties that these NMs exhibit, they are now used for a large variety of applications, and currently they are present in more than 10 400 products.[1] However, this widespread use has led to growing concern about their environmental implications and the potential risk for humans.

Silver nanoparticles or nanosilver (Ag NPs) and titanium dioxide nanoparticles or nano-titanium (TiO$_2$ NPs) are nowadays the most widely used NPs. Nanosilver exhibits antibacterial, antiviral, antifungal and anti-inflammatory characteristics, and these properties, as well as the ability to promote wound healing, have been exploited for medical and biomedical purposes including drug delivery, orthopedics, pharmaceutics, and dentistry.[2–4] Furthermore, Ag NPs are included in many daily consumer products such as cosmetics, deodorants, toothpaste, food packaging, toys, and textiles, as well as in goods from the bioelectronics industry.[5,6] Regarding nano-titanium, the main applications are focused on cosmetic preparations and personal care products (foundations, day creams, and lip balms)[7] because of their high refraction index[8] (an estimated 25% of the total nano-TiO$_2$ market is used for sunscreen formulations[9]). In addition, TiO$_2$ NPs also find applications in agriculture, building engineering, sewage, and water treatment, as well as in organic synthesis as catalysts.[10,11] Although E171 (titanium dioxide) is nowadays no longer considered safe in the food industry,[12] this food additive, which can contain up to 36% of nano-titanium,[13] was also widely used to enhance the sheen and white color of certain foods, such as candies or sauces,[14] and also as a flavor enhancer for some other nonwhite foodstuffs (soups, beer, nuts and dried vegetables).[8]

Group of Trace Element, Spectroscopy and Speciation (GETEE), Institute of Materials iMATUS, Department of Analytical Chemistry, Nutrition and Bromatology, Faculty of Chemistry, Universidade de Santiago de Compostela, Avenida das Ciencias, s/n., 15782, Santiago de Compostela, Spain. E-mail: pilar.bermejo@usc.es

This journal is © The Royal Society of Chemistry 2024

J. Anal. At. Spectrom., 2024, **39**, 573–581 | **573**

The widespread use of NPs has led to their inevitable release and presence in the environment, and NPs have already been considered as emerging pollutants.[15] However, the levels of NPs in water are expected to be low and measured environmental concentrations (MECs) within the ng L^{-1} to low μg L^{-1} range have been reported of Ti- and Ag-based NPs in tap water.[16] In addition, similar concentration ranges have been also described in surface water.[17–20] From the analytical point of view, there are still major challenges to master before understanding NPs and environmental factors and their interplay. Even though a large variety of techniques are available, the existing protocols do not yet fulfill all desirable criteria, and adequate and innovative analytical approaches for the identification, characterization, and quantification of NPs in natural environments are required.

Single-particle inductively coupled plasma mass spectrometry (spICP-MS) in combination with other instrumental techniques such as electronic microscopy and light scattering techniques is a useful nanometrological tool for the determination of NPs.[21] The principle behind the single-particle mode is that only one particle is measured at a given reading time, if a sufficiently diluted sample is introduced. Assuming this, the number of counts of the recorded signal is proportional to the number of atoms in the particle, and the frequency of the pulses relates directly to the number concentration of NPs. The direct relationship between the number of counts (number of events) and the NP number concentration requires the appropriate assessment of transport efficiency (TE%), a key parameter in the equations involved in spICP-MS calculations.[22] In addition to NP number concentration, spICP-MS gives information regarding the particle size and size distribution of the measured NPs.[22,23] However, some limitations of spICP-MS lie in the lack of information regarding the shape of the NP, and in assuming that all NPs are solid and spherical in shape. Moreover, prior knowledge of the density and composition of detected NPs is required, and NP certified reference materials for TE calculation are needed when using the particle size and particle frequency approaches. Critical statements on the advantages and limitations of spICP-MS can be found in various reviews on the topic.[21,24]

An additional challenge in nanometrology is the stability of the inorganic NPs during the sample pre-treatment, a step required for isolating and/or pre-concentrating the NPs from the bulk sample. Once NPs enter natural environments, they are subjected to different transformation processes including aggregation, oxidation, dissolution, chlorination and sulfidation.[25] Hence, separation methods that do not modify the physicochemical properties of NPs are imperative, and surfactants have been investigated for NP stabilization purposes in aqueous solutions.[26–29] Therefore, the use of surfactants for assisting extractive processes of NPs could guarantee the integrity of NPs. Surfactants (triton X-100, triton X-114, and tween 80) have been used as dispersing agents in dispersive liquid–liquid microextraction (DLLME) procedures due to their dissolution capacity in polar and non-polar media (the extractant in DLLME is an organic solvent) leading to the so-called surfactant assisted dispersive liquid–liquid microextraction (SA-DLLME). As reviewed, applications have been mainly focused on preconcentrating/isolating organic compounds and metallic ions;[30–32] although some developments have been made for gold nanoparticles (Au NPs) in water[33] and TiO$_2$ NPs and zinc oxide nanoparticles (ZnO NPs) in wastewater.[34] Analytical techniques such as inductively coupled plasma optical emission spectroscopy (ICP-OES)[34] and electrothermal vaporization-inductively coupled plasma-mass spectrometry (ETV-ICP-MS)[33] have been proposed for assessing the metal amount of the isolated NPs. These techniques assess the metal content in NPs but do not determine the number of nanoparticles. Furthermore, the phenomena of degradation (ionization) and/or agglomeration of the isolated nanoparticles during the extraction process will not be detected with the use of these techniques since their detection/determination power does not distinguish the ionic metal (in solution) from the nanoparticle metal, nor the state of aggregation (agglomeration) of the NPs. More robust information regarding the stability of the isolated NPs by SA-DLLME can be obtained by using spICP-MS because the number of isolated NPs can be measured and ionization phenomena, mainly for high ionizable NPs such as Ag NPs, can be easily detected.

Therefore, the current research aims to study the potential of SA-DLLME as an extractive technique for NPs from tap water by assessing the number of NPs as well as the size distribution of NPs by spICP-MS to prove the stability of the NPs during the extractive process. A comprehensive investigation of the experimental parameters affecting the efficiency of the SA-DLLME process was carried out, and the spotlight has been put on method validation to assess the degree of stability of TiO$_2$ NPs and Ag NPs. Since agglomeration, as well as dissolution of NPs, can be influenced by the NPs' environment (sample's components), the studies have been focused on tap water.

2. Methodology

2.1. Chemicals and standards

An N8151035 reference PEG-COOH coated gold nanoparticle suspension (49.6 nm determined by TEM, 12.4 ng mL^{-1}, number particle concentration of 9.89×10^6 mL^{-1}, in aqueous 1 mM citrate) was purchased from NanoComposix (San Diego, CA, USA). Silver nanoparticles of a nominal size of 20.8 ± 3.0 nm (0.021 mg mL^{-1}, number particle concentration of 4.2×10^{11} mL^{-1}), 41 ± 5 nm (0.021 mg mL^{-1} and number particle concentration of 5.4×10^{10} mL^{-1}), and 59 ± 6 nm (0.020 mg mL^{-1} and number particle concentration of 1.8×10^{10} mL^{-1}) were also obtained from NanoComposix. Titanium dioxide nanoparticle ethanol dispersion (15 wt%) with a nominal size of 100 nm was supplied by US Research Nanomaterials (Houston, TX, USA). Diluted suspensions of inorganic NPs were prepared in ultrapure water (Milli-Q Gradient A10, Millipore Co., Bedford, USA) by accurately weighing aliquots of the commercially available suspensions after vigorously shaking for 1.0 min. Glycerol and 1,2-dichloroethane (LC Gradient) were both purchased from Merck (Darmstadt, Germany), as well as the silver standard (AgNO$_3$, 1000 mg L^{-1} Ag) and titanium standard ((NH$_4$)$_2$TiF$_6$, 1000 mg L^{-1} Ti). Triton X-114 at 2.5% (v/v) was prepared from laboratory grade Triton X-114 (Sigma-Aldrich,

574 | J. Anal. At. Spectrom., 2024, **39**, 573–581

This journal is © The Royal Society of Chemistry 2024

San Luis, MO, USA), and nitric acid (hyperpure, 69%) from Panreac (Barcelona, Spain). NexIon setup solution (10 µg L^{-1} Be, Ce, Fe, In, Li, Mg, Pb, and U in 1% HNO$_3$) was supplied by PerkinElmer (Waltham, MA, USA).

2.2. Instrumentation

A PerkinElmer NexION® 300X inductively coupled plasma mass spectrometer (Waltham, MA, USA) was used throughout. The sample introduction system consisted of a Meinhard® nebulizer and a quartz cyclonic spray chamber. Syngistix™ Nano Application software version 2.5 was used for single-particle data processing. A JEOL 2100 transmission electron microscope (TEM, operating at 200 kV) equipped with an energy dispersive X-ray spectrometer (EDS, a solid angle of 0.28 sr in HR configuration with a 50 mm^2 detector) from JEOL, Japan was used for 100 nm TiO$_2$ NP standard characterization. A Reax vortex agitator from Heidolph (Schwabach, Germany) and a Sigma Laborzentrifugen 2K15 (Osterode, Germany) centrifuge with a cooling system were used during the SADLLME process. For weighing purposes, a Mettler Toledo ML204/01 analytical balance (Columbus, OH, USA) was employed.

2.3. SA-DLLME extraction procedure

An aliquot of 10 mL of tap water was placed in a glass tube with a conical bottom and 1.0 mL of a 49 : 1 surfactant (2.5% (w/v) triton X-114)/extractant (1,2-dichloroethane) mixture was added into the sample solution. The mixture was then vortexed at 1500 rpm for 30 s forming a cloudy solution due to the dispersion of fine droplets of organic solvent into the aqueous sample. The analytes (organic extract) were later collected by centrifugation at 3500 rpm for 5.0 min, and the recovered sedimented phase was diluted to 2.0 mL with 1.0% (w/v) glycerol (optimization and validation experiments) or to 1 mL with 1.0% (w/v) glycerol (sample analysis with an enrichment factor of 10). Redissolved extracts were again vortexed before spICP-MS measurements.

2.4. Operating conditions for spICP-MS measurements

2.4.1. Instrumental conditions. The instrumental and data acquisition parameters are listed in Table 1. The standard operation mode was used for monitoring ^{49}Ti and ^{107}Ag

Table 1 Instrumental spICP-MS conditions

Parameter	Value/type/mode
Nebulizer	Meinhard
Spray chamber	Cyclonic, quartz
Cones (sampler and skimmer)	Ni
Sample flow rate (mL min^{-1})	0.155 ± 0.001
Operation mode	Standard
Isotopes monitored	^{49}Ti, ^{107}Ag
Scan time (s)	**100**
Dwell time (µs)	100 (TiO$_2$ NPs), 50 (Ag NPs)
Mass (amu)	48.948 (TiO$_2$ NPs), 106.905 (Ag NPs)
Density (g cm^3)	4.23 (TiO$_2$ NPs), 10.49 (Ag NPs)
Mass fraction (%)	59.9 (TiO$_2$ NPs), 100 (Ag NPs)

isotopes. The choice of the most abundant isotope for Ti (^{48}Ti) was discarded because of the potential isobaric interference derived from ^{48}Ca. Measurements based on ^{49}Ti have been found to be sensitive enough when assessing Ti in complex samples.[35–39]

A tuning solution containing Be, Ce, Fe, In, Li, Mg, Pb, and U (1.0 µg L^{-1}) and Ag or Ti (10 µg L^{-1}) was used to adjust the ICP-MS prior to analysis. The flow rate was daily determined by weighing the amount of deionized ultrapure water aspirated by the sample introduction system for 1.0 min (measurements in triplicate).

2.4.2. Assessment of transport efficiency. Transport efficiency (TE%), defined as the ratio of the amount of analyte reaching the plasma compared to the amount of analyte aspirated by the sample introduction system, is one of the most critical parameters and its determination is crucial for an accurate NP quantification and size measurement. This parameter has been assessed by the pulse frequency method described by Pace *et al.*,[40] which required the daily determination of the flow rate and the analysis of a reference material of nanoparticles of certified (known) particle number concentration and size. Daily flow rate assessment gave a mean flow rate of 0.1548 ± 0.0098 mL min^{-1} values, which, together with the analysis of a gold nanoparticle suspension (nominal concentration of 9.89 × 10^4 NPs mL^{-1} and mean size of 49.6 nm), led to a mean TE% of 5.4 ± 0.7.

2.4.3. Calibration. Considering the lack of certified reference materials for the analysis of TiO$_2$ NPs and Ag NPs, dissolved standard calibration must be used. This strategy was firstly described by Pace *et al.*[40] and it requires the knowledge of the accurate value of TE% for assuming that the behavior of dissolved metal and NPs in the plasma (vaporization, atomization, and ionization) is the same. Mass calibration curves were subsequently obtained by covering the 0–10 µg L^{-1} range for both Ti and Ag measurements.

3. Results and discussion

3.1. Optimization of the SA-DLLME experimental parameters

As previously commented, NP agglomeration and/or dissolution are dependent on NPs' environment (sample's matrix). Therefore, tap water was selected for developing the SA-DLLME procedure and for a further method validation.

The effect of the main parameters affecting the extraction efficiency of the SA-DLLME process was investigated. All experiments were performed using 10 mL aliquots from tap water spiked with 25 µg L^{-1} of 100 nm TiO$_2$ NPs and 1.08 × 10^5 Ag NPs (40 nm) L^{-1} for ensuring a right measurement of TiO$_2$ NP and Ag NP events by spICP-MS. Each set of conditions was tested in triplicate and reagent blanks (10 mL of ultrapure water) were also analyzed for each case. Analytical recovery (mass concentration as TiO$_2$ µg L^{-1} for TiO$_2$ NPs and Ag NP number concentration L^{-1} for Ag NPs) was used as analytical response in optimization experiments.

Triton X-114 was selected as a surfactant,[33,34] and several preliminary experiments were performed for selecting the best

This journal is © The Royal Society of Chemistry 2024

J. Anal. At. Spectrom., 2024, **39**, 573–581 | 575

extractant, the concentration of triton X-114, and the surfactant-extractant ratio (49 : 1). A proper cloudy solution was observed when using 1,2-dichloroethane as an extractant,[33] Triton X114 at 2.5% (m/v), and a 2.5% (m/v) triton X-114/1,2-dichloroethane (49 : 1) mixture, whereas other surfactant concentrations and/or surfactant/extractant ratios led to transparent solutions and lack of a sedimented phase after centrifugation. In addition, a previous mixture of both reagents (2.5% (m/v) triton X-114/1,2-dichloroethane) before addition to the water sample was needed, since the addition of dispersant and extractant separately did not lead to cloudy dispersion. These findings agree with those reported by Selahle and Nomngongo[34] when using the triton X-114/n-butyl acetate mixture.

3.1.1. Effect of the volume of the 49 : 1 triton X-114/1,2-dichloroethane mixture. The volume of the sedimented phase is directly affected by both the volume of extractant and the volume of surfactant, as well as the volume of the sample.[41] An adequate volume of the sedimented phase is needed for ensuring a good enrichment factor (EF). Consequently, the volume of the 49 : 1 triton X-114/1,2-dichloroethane mixture was studied at 625 μL, 750 μL, and 1000 μL. The experiment was performed by vortexing at 2000 rpm for 1.0 min, and by isolating the organic phase by centrifugation at 2500 rpm and 4 °C for 3.0 min. The results (Fig. 1(a)) imply slightly higher extraction efficiencies when using 750 and 1000 μL of the surfactant/extractant mixture, achieving more repeatable results when 1000 μL was used for the extraction of TiO$_2$ NPs. Measured ionic Ti was found to be within the 0.40–0.70 μg L^{-1} range, whereas ionic Ag varied in the 0.40 to 0.60 μg L^{-1} range. Regarding size distribution (Table 2), a mean size of 36 nm was measured for Ag NPs under all conditions (water samples were previously spiked with 41 ± 5 nm Ag NPs), which implies that agglomeration and ionization processes are not observed during the extraction process. However, mean sizes for TiO$_2$ NPs were close to 200 nm, which suggests TiO$_2$ NP agglomeration since water was spiked with 100 nm TiO$_2$ NPs.

Therefore, a volume of 1000 μL of 49 : 1 triton X-114/1,2-dichloroethane mixture was selected for further experiments. The need for using large dispersant/extractant volumes has been also reported for the triton X-114/n-butyl acetate system,[34] and it contrasts to the low dispersant and extractant volumes reported by Liu *et al.* (50 and 70 μL of dispersant and extractant, respectively, in sequential addition).[33]

3.1.2. Effect of vortex (extraction) time and speed. Stirring time is a factor that influences the extraction efficiency because it influences how fast the equilibrium state is achieved. Once the mixture of the surfactant and extractant is injected into the sample, a cloudy solution is formed. Then, the mixture is gently shaken to speed up the mass transfer of the analytes from the aqueous to the organic phase. In this study, the influence of the vortex time within the 0.5–5.0 min range was tested by using a volume of 1000 μL of the 49 : 1 triton X-114/1,2-dichloroethane mixture, and fixing the vortex speed at 2000 rpm and the centrifugation conditions at 2500 rpm and 4 °C for 3.0 min.

Results plotted in Fig. 1(b) show a slight decrease in the analytical recovery of TiO$_2$ NPs for vortexing times higher than 0.5 min, whereas the extracted amounts of Ag NPs remain
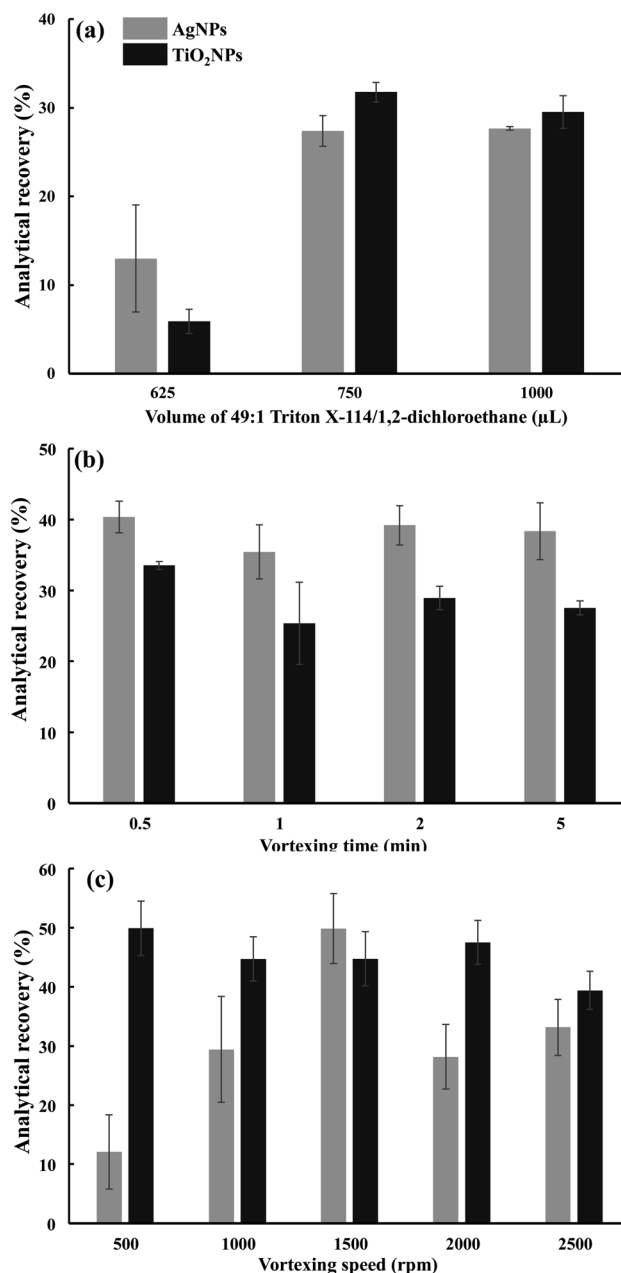

Fig. 1 Effect of the volume of 49 : 1 triton X-114/1,2-dichloroethane (a), vortexing time (b) and vortexing speed (c) on the analytical recovery of Ag NPs and TiO$_2$ NPs.

constant. The highest extraction efficiency for both NPs was achieved when using the shortest extraction time (0.5 min), which was finally selected for further studies. Ionic Ti and Ag were below 0.6 μg L^{-1} for all experiments, which suggests that the vortexing time does not lead to NP dissolution. Regarding size distribution, Table 2 lists the mean sizes for Ag NPs and TiO$_2$ NPs under all operational SA-DLLME conditions. Sizes of 36 nm were measured for Ag NPs (tap water samples spiked with 41 ± 5 nm Ag NPs), whereas mean sizes for TiO$_2$ NPs were close to 200 nm (tap water samples spiked with 100 nm TiO$_2$ NPs). These sizes are higher than the calculated size detection limits by using the 5σ criteria (see section 3.2.2), which were 65.8 nm

576 | *J. Anal. At. Spectrom.*, 2024, **39**, 573–581

This journal is © The Royal Society of Chemistry 2024

Table 2 Mean sizes of AgNPs and TiO$_2$NPs under several operational conditions

	Mean size of Ag NPs (nm)	Mean size of TiO$_2$ NPs (nm)
Volume of 49 : 1 triton X-114/1,2-dichloroethane mixture		
625 μL	36 ± 3	207 ± 9
750 μL	36 ± 1	205 ± 3
1000 μL	36 ± 1	196 ± 5
Vortexing time		
0.5 min	32 ± 3	226 ± 19
1.0 min	37 ± 1	231 ± 17
2.0 min	38 ± 1	232 ± 4
5.0 min	38 ± 1	241 ± 11
Vortexing speed		
500 rpm	30 ± 2	318 ± 9
1000 rpm	36 ± 1	315 ± 3
1500 rpm	35 ± 1	314 ± 3
2000 rpm	24 ± 1	314 ± 5
2500 rpm	25 ± 1	299 ± 1
Centrifugation speed		
2000 rpm	37 ± 4	212 ± 3
2500 rpm	35 ± 2	221 ± 7
3000 rpm	31 ± 3	218 ± 4
3500 rpm	33 ± 1	218 ± 3
Centrifugation time		
1 min	31 ± 1	228 ± 7
3 min	39 ± 3	252 ± 2
5 min	40 ± 2	246 ± 5
10 min	39 ± 1	242 ± 8

and 16.7 nm for TiO$_2$ NPs and Ag NPs, respectively. Since mean sizes obtained for Ag NPs (36 nm) are close to the nominal size of the Ag NP standard used for spiking (41 ± 5 nm), we can conclude that the stability of Ag NPs is guaranteed during the SA-DLLME procedure. However, the higher sizes measured for TiO$_2$ NPs (close to 200 nm) suggest TiO$_2$ NP agglomeration (TiO$_2$ NP standard of 100 nm), but conclusions regarding TiO$_2$ NP stability d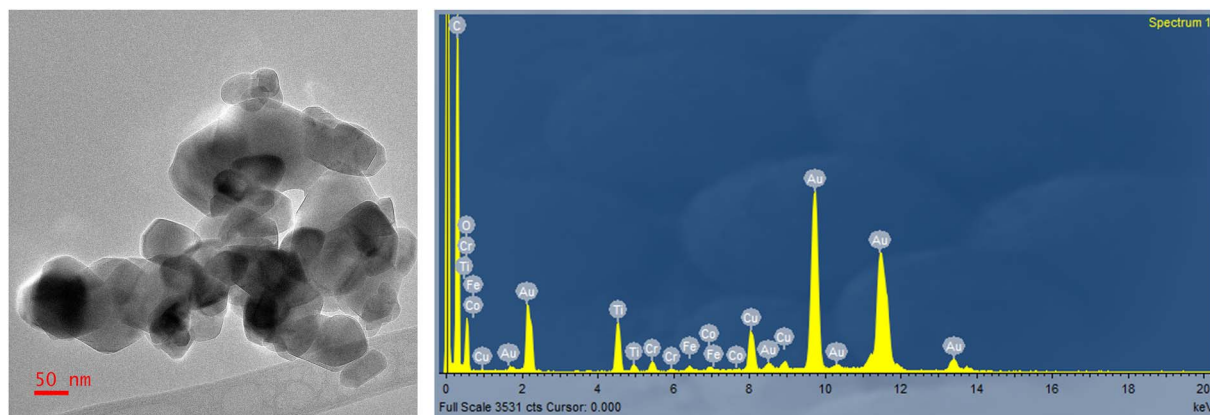uring the SA-DLLME process cannot be attained since the direct analysis of the 100 nm TiO$_2$ NP standard by transmission electron microscopy (Fig. 2) shows large TiO$_2$ NP aggregates.

Like the time of vortexing, the vortexing speed influences the equilibrium between the donor and the acceptor phases, and consequently, the mass transfer of analytes. The selection of the vortexing speed was limited to the operational range of the vortex device used, and so the influence was studied within the 500–2500 rpm range. Previously selected conditions for 49 : 1 triton X-114/1,2-dichloroethane mixture volume (1000 μL) and vortex time (0.5 min), as well as fixed centrifugation conditions (2500 rpm and 4 °C for 3.0 min), were used throughout the experiment.

The results in Fig. 1(c) show that the stirring speed does not have an apparent effect on TiO$_2$ NP extraction, but Ag NP extraction efficiency is improved when vortexing at moderate speeds (1500 rpm). These findings imply a better Ag NP transfer at moderate speeds and the decrease in Ag NP recovery at higher speeds could be attributed to Ag NP ionization (low mean sizes at high vortexing speed as listed in Table 2). Therefore, a vortexing speed of 1500 rpm was finally selected for an efficient simultaneous co-extraction of Ag NPs and TiO$_2$ NPs.

3.1.3. Effect of centrifugation speed and time. Centrifugation is a critical step during the SA-DLLME process due to potential losses of NPs by dissolution and/or agglomeration. Centrifugation is used to speed up phase separation and thus, speed and time need to be carefully investigated. Centrifugation speeds ranging from 2000 to 3500 rpm were tested, and the results are shown in Fig. 3(a). It can be observed that higher centrifugation speeds promote higher extraction efficiencies for both TiO$_2$ NPs and Ag NPs, and 3500 rpm was finally selected as the speed of choice for the centrifugation step.

The effect of centrifugation time was tested within the 1.0–10 min range (centrifugation speed at 3500 rpm and vortex conditions at optimum values, section 3.1.2). Fig. 3(b) shows higher extraction efficiencies when increasing the centrifugation time, and the highest extraction efficiency for TiO$_2$ NPs is already obtained within the 3.0–5.0 min range; meanwhile, the highest extraction for Ag NPs is achieved at times longer than 5.0 min. Differences in the centrifugation time for both types of

Fig. 2 TEM image and EDS spectra of the 100 nm TiO$_2$ NP standard.

This journal is © The Royal Society of Chemistry 2024

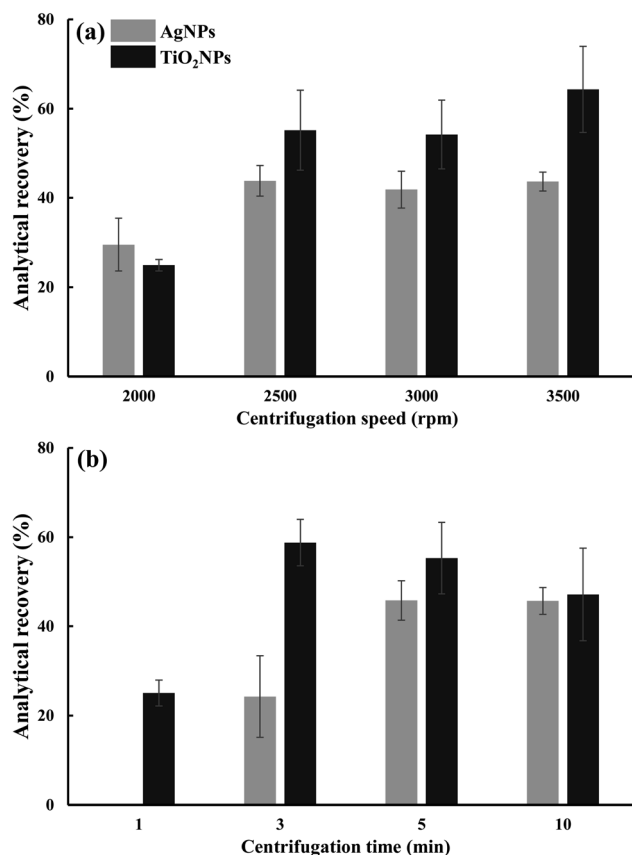*J. Anal. At. Spectrom.*, 2024, **39**, 573–581 | **577**

Fig. 3 Effect of the centrifugation speed (a) and centrifugation time (b) on the analytical recovery of Ag NPs and TiO$_2$ NPs.

NPs can be explained by the different sedimentation speeds of each one, a parameter mathematically described by the Svedberg equation[42] and is directly dependent on the density and the radius of the particle:

$$\frac{\mathrm{d}x/\mathrm{d}t}{\omega^2 x} = \frac{2r^2 \left(\rho_\mathrm{p} - \rho_\mathrm{m}\right)}{9\eta}$$

where ω is the angular velocity, x the distance from the rotational axis, r the radius of the particle, ρ_p and ρ_m the densities of the particle and the medium respectively, and η the viscosity.

For a joint extraction, centrifugation of the cloudy solution for 5.0 min will be considered as the optimal time. As listed in Table 2, the mean sizes of Ag NPs were close to 40 nm under all conditions, whereas the mean sizes for TiO$_2$ NPs varied from 228 to 252 nm.

3.2. Analytical performance

3.2.1. Calibration and matrix effect. In order to verify the presence or absence of the matrix effect, a series of aqueous ionic calibrations (Ag and Ti concentrations within the 0–10 μg L^{-1} range) were performed and the slopes were statistically compared with those obtained by preparing ionic standards (same concentrations) but using reconstituted (2.0 mL with 1% (w/v) glycerol) sedimented phases obtained after applying the SA-DLLME procedure to 10 mL aliquots of ultrapure water

(matrix matched calibration). Counts *versus* μg event^{-1} were plotted and, in all cases, $r^2 > 0.997$ was achieved. The statistical analysis (90% confidence interval) revealed that there are statistically significant differences (p-value < 0.1) between the slopes of the aqueous ionic calibration (8.0×10^9 counts events μg^{-1}) and the matrix matched calibration (1.0×10^{10} counts events μg^{-1}) for Ti. However, p-values > 0.1 were obtained when comparing the calibration slopes of Ag (9.0×10^{10} and 1.0×10^{11} counts events μg^{-1} for the aqueous ionic calibration and matrix matched calibration, respectively); hence, there were not statistically significant differences between the slopes of both calibration modes. These findings imply that there is no matrix effect for Ag, but the reagents used for SA-DLLME promote matrix effects when measuring Ti.

3.2.2. Limits of detection and limits of quantification. The detection capabilities of spICP-MS are related not only to concentration but also to the mass of element per particle, which can be translated into particle size. Therefore, two LODs must be considered, a size detection limit (LOD$_{\text{SIZE}}$) and a nanoparticles number concentration limit of detection (LOD$_{\text{NP}}$). The assessment of these features has been performed by applying the calculation Excel tool designed by Laborda *et al.*[43] based on the 3σ ($3 \times$ baseline standard deviation) and 5σ ($5 \times$ baseline standard deviation) criterion.

Table 3 lists the several outputs for number concentration and size, and for dissolved mass concentration (critical value and limit of detection) assessed. The number concentration critical values were 2.67×10^6 NPs L^{-1}, and 5.84×10^6 L^{-1} for TiO$_2$ NPs and Ag NPs, respectively. The number concentration limits of detection were 2.85×10^6 NPs L^{-1} (TiO$_2$ NPs) and 6.06×10^6 L^{-1} (Ag NPs), which after assuming an EF of 10 led to a number concentration limit of detection referred to the tap water of 2.85×10^5 NPs L^{-1} for TiO$_2$ NPs and 6.06×10^5 L^{-1} for Ag NPs. Table 3 also lists the dissolved mass concentration (critical value and limit of detection), values within the 2.94–5.38 ng L^{-1} range for Ti, and from 0.238 to 0.435 ng L^{-1} for Ag.

Regarding the limit of detection in size, values of 65.8 (5σ criteria) and 55.5 nm (3σ criteria) were assessed for TiO$_2$ NPs, whereas the minimum sizes for Ag NPs were 16.7 (5σ criteria) and 14.1 nm (3σ criteria). These values imply a mass per particle limit of detection of 631.6 ag (5σ criteria) and 379.0 ag (3σ criteria) for TiO$_2$ NPs; and a mass per particle limit of detection of 25.49 ag (5σ criteria) and 15.30 ag (3σ criteria) for Ag NPs. Since the use of a criterion higher than 4σ virtually eliminates the occurrence of false positives when nanoparticle distributions are partially overlapped with the background,[44] the 5σ criterion was selected for establishing the size limit of detection (Table 3). These values match with reported LODs in size by other authors (13–30 nm for Ag NPs and 50–100 nm for TiO$_2$ NPs).[45–47]

3.2.3. Selectivity of the SA-DDLME procedure for nanoparticle forms of Ti and Ag. The selectivity of the method (the ability of the SA-DLLME procedure for isolating TiO$_2$ NPs and Ag NPs in the presence of ionic Ti and Ag) was tested by subjecting 10 mL aliquots of ionic Ti (25 μg L^{-1}) and Ag (8.0 μg L^{-1}) solutions to the proposed SA-DLLME procedure. Experiments in triplicate showed very low analytical recoveries (4.2 ± 2.4% and

Table 3 Number concentration and size limit of detection of the method

		3σ criteria		5σ criteria	
		Critical value	Limit of detection	Critical value	Limit of detection
TiO$_2$ NPs	Number concentration/L^{-1}	2.67×10^6	2.85×10^{6a}	2.67×10^6	2.85×10^{6a}
	Dissolved mass concentration/ng L^{-1}	2.94	5.38	2.94	5.38
	Size/nm	55.5	55.5	65.8	65.8
	Mass per particle/ag	379.0	379.0	631.6	631.6
Ag NPs	Number concentration/L^{-1}	5.84×10^6	6.06×10^{6b}	5.84×10^6	6.06×10^{6b}
	Dissolved mass concentration/ng L^{-1}	0.238	0.435	0.238	0.435
	Size/nm	14.1	14.1	16.7	16.7
	Mass per particle/ag	15.3	15.3	25.5	25.5

[a] 2.85×10^5 L^{-1} (referred to the tap water sample, EF 10). [b] 6.06×10^5 L^{-1} (referred to the tap water sample, EF 10).

2.5 ± 0.1% for dissolved Ti and Ag, respectively). In this way, SA-DLLME proves to be selective for isolating nanoparticle forms of Ti and Ag.

3.2.4. Analytical recovery assays. The accuracy of the spICP-MS measurement was studied through the analytical recovery by combining several extracts from a tap water after applying the proposed SA-DLLME, and spiking extract aliquots with 20 and 60 nm Ag NPs at 6.0×10^4 and 12×10^4 mL^{-1}; and with 100 nm TiO$_2$ NPs at 25 and 50 µg L^{-1} (experiments in triplicate for each NP and concentration level). Analytical recovery values were calculated by subtracting the un-spiked concentration values from the spiked extracts and dividing them by the standard concentration used for spiking experiments. As listed in Table 4, analytical recoveries within the 80–120% range were obtained for all cases, which implies good accuracy for the spICP-MS measurement process.

Similarly, the accuracy of the over-all method (SA-DLLME and spICP-MS) was also assessed through the analytical recovery after applying the SA-DLLME procedure to water samples spiked with Ag NPs of two size distributions (40 and 60 nm) at two concentration levels (6.0×10^4 and 12×10^4 mL^{-1}, each one), and with 100 nm TiO$_2$ NPs at 25 and 50 µg L^{-1} each one. Spiked and un-spiked samples, as well as NP standards, were measured in triplicate. Analytical recovery, also calculated by subtracting the un-spiked concentration values from the spiked extracts and using the standard concentrations for spiking experiments as a reference, is listed in Table 4. The obtained TiO$_2$ NP analytical recoveries ranged from 47 ± 5 to 58

± 3%, whereas the analytical recoveries obtained for Ag NPs were between 44 ± 4 and 53 ± 7%. A representative histogram for spiked experiments with 100 nm TiO$_2$ NPs (50 µg L^{-1}) is given in Fig. 4(a), showing TiO$_2$ NP sizes larger than 100 nm because of the agglomeration phenomena. In the case of Ag NPs (40 nm, 12×10^4 mL^{-1}), a size distribution close to the nominal size (40 nm) was observed (Fig. 4(b)) together with an additional size distribution (sizes lower than 25 nm) related to Ag NPs close to the LOD$_{SIZE}$ (lower than 16.7 nm, 5σ criteria) and ionic silver. In general, dissolved titanium and silver concentrations were found to be lower than 0.80 µg L^{-1} which could imply that the SA-DLLME procedure is a safe methodology for guaranteeing the integrity of Ag NPs and TiO$_2$ NPs.

The low analytical recovery assessed when considering the over-all process (SA-DLLME and spICP-MS) is attributed to the equilibrium achieved with the SA-DLLME procedure, which implies analytical recoveries around 50%. Several experiments were further performed for verifying the non-exhaustive nature of the SA-DLLME process. The first set of experiments consisted of subjecting the residues (tap water) after carrying out the SA-DLLME (first extraction) to a second SA-DLLME (second successive extraction), obtaining analytical recoveries for Ag NP trials of 44 ± 5 and 41 ± 4% (40 nm Ag NPs at 6.0×10^4 and 12×10^4 mL^{-1}, respectively), and 58 ± 4 and 44 ± 5% (60 nm Ag NPs at 6.0×10^4 and 12×10^4 mL^{-1}, respectively). Additionally, new spiking experiments for Ag NPs were also developed but using lower Ag NP number concentrations (3.0×10^4 mL^{-1}) and

Table 4 Analytical recovery of the spICP-MS measurements and of the over-all procedure (SA-DLLME and spICP-MS)

		spICP-MS			SA-DLLME – spICP-MS	
		Added concentration	Analytical recovery[a] (%)		Added concentration	Analytical recovery[a] (%)
Ag NPs	20 nm	6.0×10^4 mL^{-1}	96 ± 6	40 nm	6.0×10^4 mL^{-1}	44 ± 4
		12×10^4 mL^{-1}	114 ± 4		12×10^4 mL^{-1}	53 ± 7
	60 nm	6.0×10^4 mL^{-1}	83 ± 5	60 nm	6.0×10^4 mL^{-1}	50 ± 5
		12×10^4 mL^{-1}	99 ± 6		12×10^4 mL^{-1}	47 ± 5
TiO$_2$ NPs	100 nm	25 µg L^{-1}	104 ± 7	100 nm	25 µg L^{-1}	58 ± 3
		50 µg L^{-1}	88 ± 3		50 µg L^{-1}	47 ± 5

[a] $n = 3$.

This journal is © The Royal Society of Chemistry 2024
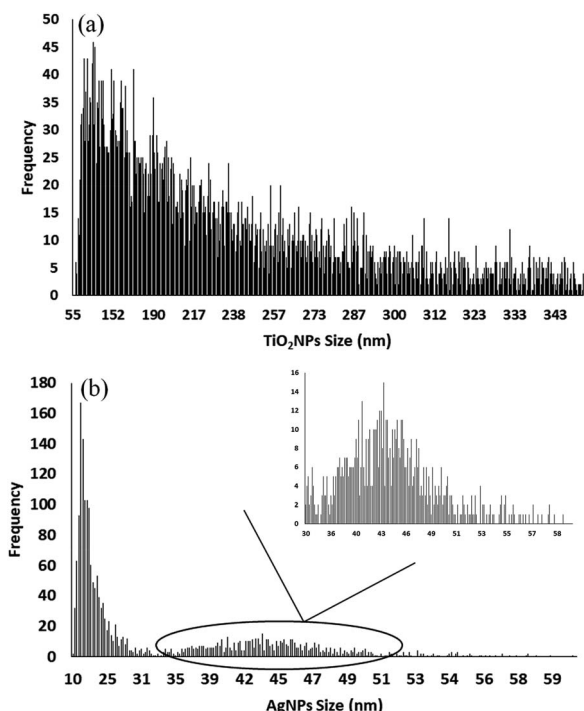
J. Anal. At. Spectrom., 2024, **39**, 573–581 | **579**

Fig. 4 Representative histograms for extracts from a tap water sample spiked with 50 μg L^{-1} of 100 nm TiO$_2$ NPs (a) and 12×10^4 mL^{-1} of 40 nm Ag NPs (b).

similar analytical recoveries (44 ± 3 and $51 \pm 4\%$ for 40 nm Ag NPs and 60 nm Ag NPs, respectively) were also obtained.

Therefore, a procedural standard calibration consisting of the use of Ag NPs/TiO$_2$ NPs at increasing concentrations subjected to the SA-DLLME must be used to assess accurate results (quantitative analytical recoveries).

4. Conclusions

Pre-concentration procedures based on SA-DLLME are reliable sample pre-treatments for assessing Ag NPs and TiO$_2$ NPs in tap water. The procedure has been found to be selective for nanoparticle titanium and silver forms (ionic Ag and Ti species are not extracted), and the enrichment factor (5–10) could be improved, when necessary, by using large volumes of sample. Therefore, the SA-DLLME technique can be used as sample pre-treatment for the determination of Ag NPs and TiO$_2$ NPs by instrumental techniques such as ICP-OES/MS and others because the selective isolation of the nanoparticle forms is achieved. In addition, NP dissolution did not occur during the extraction process since spICP-MS analysis has revealed very low ionic titanium and silver concentrations in the extracts. However, spiking experiments for TiO$_2$ NPs have shown agglomeration since TiO$_2$ NP sizes higher than the nominal sizes of the TiO$_2$ NPs used for spiking were observed. Moreover, SA-DLLME is a technique based on the equilibrium of the targets between the donor (sample) and the acceptor (extract) phases, and a procedural standard calibration has therefore

been required for assessing accurate results. Finally, although the current research has been focused on tap water, the developed SA-DLLME methodology offers potential applications to other more complex water samples such as environmental water (seawater and riverine water), wastewater, and bottled water. Further studies are needed for verifying the influence of the matrix composition of these water samples on the selectivity (nanoparticle and ionic forms) and analytical recovery when applying SA-DLLME methodologies for the isolation of Ag NPs and TiO$_2$ NPs.

Conflicts of interest

There are no conflicts to declare.

References

1 *Nanotechnology Products Database*, http://product.statnano.com (Accessed 2022 December).

2 M. Murphy, K. Ting, X. Zhang, C. Soo and Z. Zheng, *J. Nanomater.*, 2015, **2015**, 5, DOI: 10.1155/2015/696918.

3 S. J. Soenen, W. J. Parak, J. Rejman and B. Manshian, *Chem. Rev.*, 2015, **115**, 2109–2135, DOI: 10.1021/cr400714j.

4 L. Rizzello and P. P. Pompa, *Chem. Soc. Rev.*, 2014, **43**, 1501–1518, DOI: 10.1039/c3cs60218d.

5 B. A. Weldon, E. M. Faustman, G. Oberdörster, T. Workman, W. C. Griffith, C. Kneuer and I. J. Yu, *Nanotoxicology*, 2016, **10**, 945–956, DOI: 10.3109/17435390.2016.1148793.

6 A. Haider and I. K. Kang, *Adv. Mater. Sci. Eng.*, 2015, **2015**, 65257, DOI: 10.1155/2015/165257.

7 B. Dréno, A. Alexis, B. Chuberre and M. Marinovich, *J. Eur. Acad. Dermatol. Venereol.*, 2019, **33**, 34–46, DOI: 10.1111/jdv.15943.

8 R. J. B. Peters, G. Van Bemmel, Z. Herrera-Rivera, H. P. F. G. Helsper, H. J. P. Marvin, S. Weigel, P. C. Tromp, A. G. Oomen, A. G. Rietveld and H. Bouwmeester, *J. Agric. Food Chem.*, 2014, **62**, 6285–6293, DOI: 10.1021/jf5011885.

9 S. Heilgeist, R. Sekine, O. Sahin and R. A. Stewart, *Water*, 2021, **13**, 734, DOI: 10.3390/w13050734.

10 E. Baranowska-Wójcik, D. Szwajgier, P. Oleszczuk and A. Winiarska-Mieczan, *Biol. Trace Elem. Res.*, 2020, **193**, 118–129, DOI: 10.1007/s12011-019-01706-6.

11 M. S. Waghmode, A. B. Gunjal, J. A. Mulla, N. N. Patil and N. N. Nawani, *SN Appl. Sci.*, 2019, **1**, 310, DOI: 10.1007/s42452-019-0337-3.

12 European Food Safety Agency, *Titanium Dioxide: E171 No Longer Considered Safe when Used as a Food Additive*. https://www.efsa.europa.eu/en/news/titanium-dioxide-e171-no-longer-considered-safe-when-used-food-additive (Accessed December 2022).

580 | *J. Anal. At. Spectrom.*, 2024, **39**, 573–581

This journal is © The Royal Society of Chemistry 2024

13 Y. Yang, K. Doudrick, X. Bi, K. Hristovski, P. Herckes, P. Westerhoff and R. Kaegi, *Environ. Sci. Technol.*, 2014, **48**, 6391–6400.

14 W. Mu, Y. Wang, C. Huang, Y. Fu, J. Li, H. Wang, X. Jia and Q. Ba, *J. Agric. Food Chem.*, 2019, **67**, 9382–9389, DOI: **10.1021/acs.jafc.9b02391**.

15 B. F. da Silva, S. Pérez, P. Gardinalli, R. K. Singhal, A. A. Mozeto and D. Barceló, *Trends Anal. Chem.*, 2011, **30**, 528–540, DOI: **10.1016/j.trac.2011.01.008**.

16 J. Zhao, M. Lin, Z. Wang, X. Cao and B. Xing, *Crit. Rev. Environ. Sci. Technol.*, 2021, **51**, 1443–1478, DOI: **10.1080/10643389.2020.1764279**.

17 L. J. A. Ellis, M. Baalousha, E. Valsami-Jones and J. R. Lead, *Chemosphere*, 2018, **191**, 616–625, DOI: **10.1016/j.chemosphere.2017.10.006**.

18 L. Li, M. Sillanpää and M. Risto, *Environ. Pollut.*, 2016, **219**, 132–138, DOI: **10.1016/j.envpol.2016.09.080**.

19 Z. X. Luo, Z. H. Wang, B. Xu, I. L. Sarakiotis, G. Du Laing and C. Z. Yan, *J. Zhejiang Univ., Sci., A*, 2014, **15**, 593–605, DOI: **10.1631/jzus.A1400111**.

20 F. Gottschalk, T. Sun and B. Nowack, *Environ. Pollut.*, 2013, **181**, 287–300, DOI: **10.1016/j.envpol.2013.06.003**.

21 F. Laborda, E. Bolea, G. Cepriá, M. T. Gómez, M. S. Jiménez, J. Pérez-Arantegui and J. R. Castillo, *Anal. Chim. Acta*, 2016, **904**, 10–32, DOI: **10.1016/j.aca.2015.11.008**.

22 F. Laborda, J. Jiménez-Lamana, E. Bolea and J. R. Castillo, *J. Anal. At. Spectrom.*, 2011, **26**, 1362–1371, DOI: **10.1039/c0ja00098a**.

23 T. A. Saleh, *Trends Environ. Anal. Chem.*, 2020, **28**, 1–10, DOI: **10.1016/j.teac.2020.e00101**.

24 D. Mozhayeva and C. Engelhard, *J. Anal. At. Spectrom.*, 2020, **35**, 1740–1783, DOI: **10.1039/c9ja00206e**.

25 G. R. Tortella, O. Rubilar, N. Durán, M. C. Diez, M. Martínez, J. Parada and A. B. Seabra, *J. Hazard. Mater.*, 2020, **390**, 121974, DOI: **10.1016/j.jhazmat.2019.121974**.

26 X. Du, X. Wang, S. You, Q. Wang and X. Gong, *J. Environ. Sci.*, 2015, **36**, 84–92, DOI: **10.1016/j.jes.2015.05.011**.

27 K. Raja, P. S. Ramesh, D. Geetha, T. Kokila and R. Sathiyapriya, *Spectrochim. Acta, Part A*, 2015, **136**, 155–161, DOI: **10.1016/j.saa.2014.08.092**.

28 I. G. Godinez and C. J. G. Darnault, *Water Res.*, 2011, **45**, 839–851, DOI: **10.1016/j.watres.2010.09.013**.

29 I. G. Godinez, C. J. G. Darnault, A. P. Khodadoust and D. Bogdan, *Environ. Pollut.*, 2013, **174**, 106–113, DOI: **10.1016/j.envpol.2012.11.002**.

30 A. Spietelun, Ł. Marcinkowski, M. de la Guardia and J. Namieśnik, *Talanta*, 2014, **119**, 34–45, DOI: **10.1016/j.talanta.2013.10.050**.

31 V. Azevedo Lemos, J. Alves Barreto, L. Bastos Santos, R. dos Santos de Assis, C. Galvão Novaes and R. J. Cassella, *Talanta*, 2022, **238**, 123002, DOI: **10.1016/j.talanta.2021.123002**.

32 I. Hagarová, L. Nemček, M. Šebesta, O. Zvěřina, P. Kasak and M. Urík, *Int. J. Mol. Sci.*, 2022, **23**, 11465, DOI: **10.3390/ijms231911465**.

33 Y. Liu, M. He, B. Chen and B. Hu, *Spectrochim. Acta, Part B*, 2016, **122**, 94–102, DOI: **10.1016/j.sab.2016.04.009**.

34 S. K. Selahle and P. N. Nomngongo, *Toxicol. Environ. Chem.*, 2019, **101**, 204–214, DOI: **10.1080/02772248.2019.1686151**.

35 M. V. Taboada-López, S. Iglesias-López, P. Herbello-Hermelo, P. Bermejo-Barrera and A. Moreda-Piñeiro, *Anal. Chim. Acta*, 2018, **1018**, 16–25, DOI: **10.1016/j.aca.2018.02.075**.

36 M. V. Taboada-López, P. Herbello-Hermelo, R. Domínguez-González, P. Bermejo-Barrera and A. Moreda-Piñeiro, *Talanta*, 2019, **195**, 23–32, DOI: **10.1016/j.talanta.2018.11.023**.

37 K. Badalova, P. Herbello-Hermelo, P. Bermejo-Barrera and A. Moreda-Piñeiro, *J. Trace Elem. Med. Biol.*, 2019, **54**, 55–61, DOI: **10.1016/j.jtemb.2019.04.003**.

38 M. V. Taboada-López, G. Vázquez-Expósito, R. Domínguez-González, P. Herbello-Hermelo, P. Bermejo-Barrera and A. Moreda-Piñeiro, *Food Chem.*, 2021, **360**, 130002, DOI: **10.1016/j.foodchem.2021.130002**.

39 M. V. Taboada-López, B. H. Leal-Martínez, R. Domínguez-González, P. Bermejo-Barrera, P. Taboada-Antelo and A. Moreda-Piñeiro, *Talanta*, 2021, **233**, 122494, DOI: **10.1016/j.talanta.2021.122494**.

40 H. E. Pace, N. J. Rogers, C. Jarolimek, V. A. Coleman, C. P. Higgins and J. F. Ranville, *Anal. Chem.*, 2011, **83**, 9361–9369, DOI: **10.1021/ac201952t**.

41 M. Saraji and M. K. Boroujeni, *Anal. Bioanal. Chem.*, 2014, **406**, 2027–2066, DOI: **10.1007/s00216-013-7467-z**.

42 J. D. Castle, Overview of cell fractionation, *Curr. Protoc. Cell Biol.*, 1998, **69**, 3.1.1–3.1.9, DOI: **10.1002/0471143030.cb0301s00**.

43 F. Laborda, A. C. Gimenez-Ingalaturre, E. Bolea and J. R. Castillo, *Spectrochim. Acta, Part B*, 2020, **169**, 105883, DOI: **10.1016/j.sab.2020.105883**.

44 F. Laborda, J. Jiménez-Lamana, E. Bolea and J. R. Castillo, *J. Anal. At. Spectrom.*, 2013, **28**, 1220–1232, DOI: **10.1039/c3ja50100k**.

45 F. Laborda, E. Bolea and J. Jiménez-Lamana, *Trends Environ. Anal. Chem.*, 2016, **9**, 15–23, DOI: **10.1016/j.teac.2016.02.001**.

46 F. Laborda, E. Bolea and J. Jimenez-Lamana, *Anal. Chem.*, 2014, **86**, 2270–2278.

47 R. Peters, Z. Herrera-Rivera, A. Undas, M. Van Der Lee, H. Marvin, H. Bouwmeester and S. Weigel, *J. Anal. At. Spectrom.*, 2015, **30**, 1274–1285, DOI: **10.1039/c4ja00357h**.

This journal is © The Royal Society of Chemistry 2024

J. Anal. At. Spectrom., 2024, **39**, 573–581 | **581**